

Supplementary Information

Characterization and strong piezoelectric response of an organometallic nonlinear optical crystal:



Xitao Liu, Xinqiang Wang^{*}, Xin Yin, Shaojun Zhang, Lei Wang, Luyi Zhu, Guanghui Zhang, Dong Xu^{*}

Table 1S. Crystal data and structure refinement for CMTD

Figure 1S. Molecular structure of CMTD

Figure 2S. As grown CMTD crystals (a); factual growth morphology (b); theoretical morphology predicted by the BFDH model (c).

Figure 3S. UV-Vis-NIR transmittance spectrum of CMTD crystal.

Figure 4S. TGA/DTA curves of CMTD in air.

Table 1S. Crystal data and structure refinement for CMTD

Empirical formula	C ₈ H ₁₂ CdHgN ₄ O ₂ S ₆
Radiation λ (Mo Kα) (Å)	0.71073
Molecular weight	701.57
Temperature (K)	296(2)
Description	Prism
Color	Colorless
Crystal size (mm)	0.24 × 0.15 × 0.13
Crystal system	Orthorhombic
Crystal group	P2 ₁ 2 ₁ 2 ₁
a(Å)	8.52860(10)
b(Å)	8.5521(2)
c(Å)	28.2714(7)
V(Å ³)	2062.04(7)
Z	4
D _{cal.} (mg·m ⁻³)	2.260
Absorption coefficient (mm ⁻¹)	9.081
Absorption correction T _{min} and T _{max}	0.3848 and 0.2192
F (0 0 0)	1312
Absorption correction	Semi-empirical from equivalents
Refinement method	Full-matrix least-squares on F ²
Final R indices [I > 2 σ(I)]	R ₁ = 0.0305, wR ₂ = 0.0495
R indices (all data)	R ₁ = 0.0563, wR ₂ = 0.0553
Data/restraints/parameters	4592 / 0 / 204
Goodness-of-fit on F ²	0.876
Largest diff. peak and hole/Å ⁻³	0.742 and -0.423

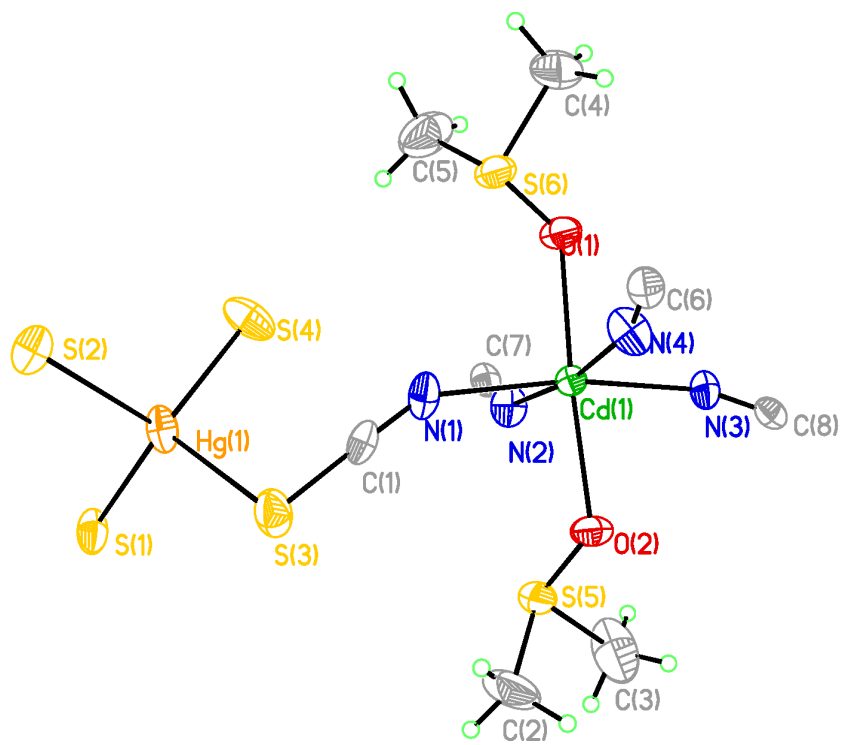
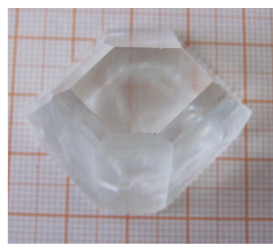
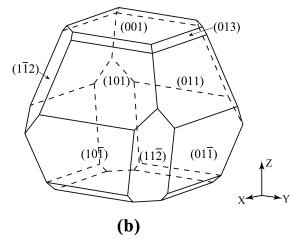


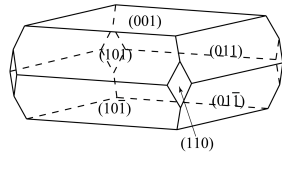
Figure 1S. Molecular structure of CMTD



(a)



(b)



(c)

Figure 2S. As grown CMTD crystals (a); factual growth morphology (b); theoretical morphology predicted by the BFDH model (c).

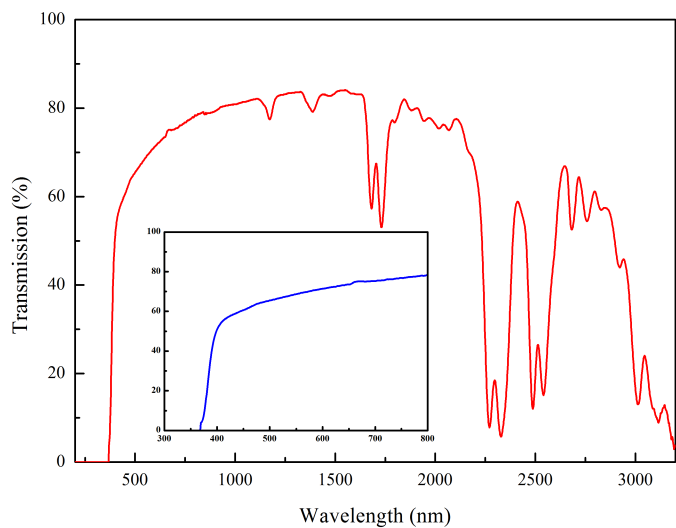


Figure 3S. UV-Vis-NIR transmittance spectrum of CMTD crystal.

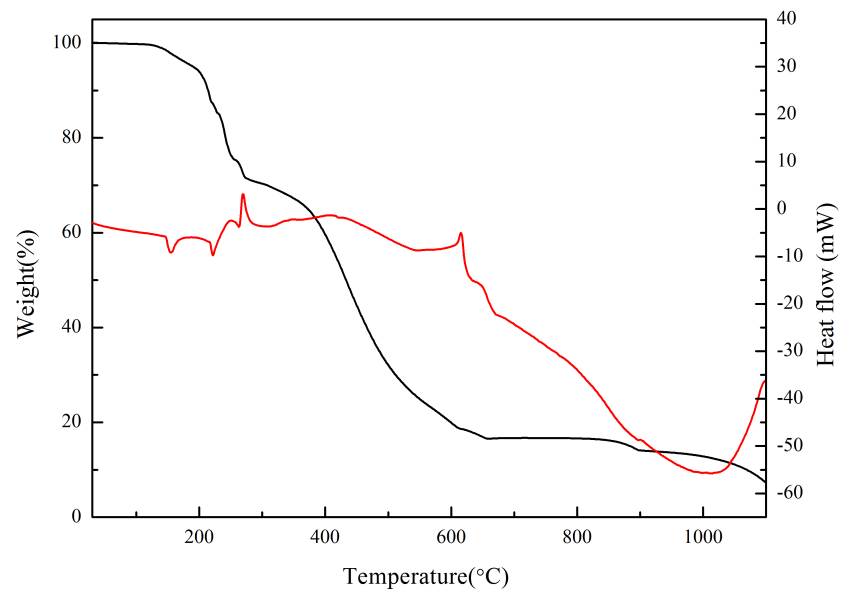


Figure 4S. TGA/DTA curves of CMTD in air.

Single-Crystal X-ray Diffraction.

A colorless and transparent crystal was selected to the desired dimensions of about $0.24 \times 0.15 \times 0.13$ mm³, which was then mounted on a glass fiber by glue to perform the data collection using a Bruker Smart Apex-II CCD diffractometer with Mo K α radiation ($\lambda = 0.71073$ Å) at 296(2) K. Preliminary lattice parameters and orientation matrices were indexed from three sets of frames. Data integration and cell refinement were carried out by the INTEGRATE program of the APEX2 software,¹ and multiscan absorption corrections were done using the SCALE program.¹ The program XPREP² provided two possible space groups: $P4_12_12$ (No. 92) and $P4_32_12$ (No. 96). While attempts to solve the structure in the two space group failed to give a reasonable solution, and the refinements were not converged. Thus, the structure was solved in the lower symmetric space group $P2_12_12_1$ (No. 18) by direct methods and refined by full-matrix least-squares fitting on F^2 by SHELX.² All non-hydrogen atoms were refined with anisotropic thermal parameters, and the refinements converged for $I > 2\sigma(I)$. All calculations were performed using the SHELXTL crystallographic software package. Structures were also checked for possible missing symmetry with PLATON.³

Crystal Growth and Morphology.

Because of wide applications of NCS materials, the size and the quality of single crystal are important, especially for crystals used in optical applications. Since they are used in laser frequency doubling, single crystals of good quality with centimeter level need to be grown.⁴ Crystals of good quality were obtained after about one month with the largest of $38 \times 33 \times 32$ mm³ as shown in Figure 2S (a).

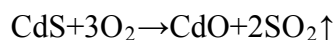
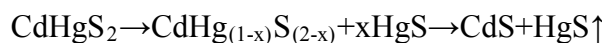
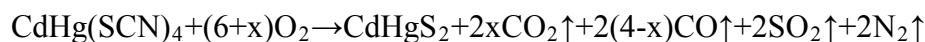
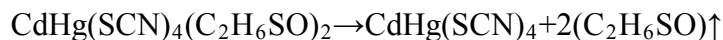
The factual morphology of the grown crystals was obtained by analyzing the diffraction data and measuring the interfacial angles in the habit (Figure 2S(b)). The {0 0 1} (the largest facet), {1 0 1}, {0 1 1}, {0 1 3}, and {1 1 2} facets were formed during the crystal growth. The theoretical morphology of CMTD crystal was also predicted by the Bravais-Friedel-Donnay-Harker (BFDH)^{5, 6} model using the Mercury program,^{7, 8} which is presented in Figure 2S(c). As we can see that there are some difference between the two morphologies which may be attributable to growth conditions such as seed orientation, solvent supersaturation, pH value, temperature, impurities, hydrodynamics, cooling rate and etc.

UV-Vis-NIR Transmittance Spectrum.

Room temperature UV-Vis-NIR transmission spectrum of CMTD crystal was recorded on the Hitachi model U-3500 recording spectrophotometer at room temperature, as shown in Figure 3S. The results indicate that the CMTD crystal presents a broad transmission range from 360 to 2270 nm and its ultraviolet(UV) transparency cutoff occurs at 360 nm (3.451 eV) which shows 12 nm hypsochromic shift compared with that of CMTC crystal.⁹ The hypsochromic shift can be attributed to the metal-to-ligand charge-transfer (MLCT), ligand-to-metal charge-transfer (LMCT) or metal-mediated ligand transition. When DMSO is introduced into CMTC, the coordination of two O atoms to Cd ions, which increases the Cd-to-DMSO charge-transfer and reduces metal-to-SCN charge-transfer, results in the hypsochromic shift.

Thermal Properties.

Thermogravimetric (TG) and differential thermal analysis (DTA) of CMTD measurements in air were performed on a Diamond TG/DTA Perkin-Elmer instrument in air with a heating rate of flux 10 °C/min from 30 to 1100 °C. The plots are shown in Figure 4S. Some thermoanalytical data of CMTD crystal has been reported in the literature.¹⁰ The decomposition process is not a single stage but consists of four steps. The results show that the sample starts decomposing at about 150 °C, the loss of the ligand molecule DMSO, corresponding to an endothermic peak in the DTA curve. The following thermal processes are the same as those of CMTC.¹¹ Through analysis the main possible reactions of thermal decomposition (in air) of CMTD can be expressed as follows:



The results indicate that the thermal stability of CMTD (150°C) is lower than that of CMTC (202.9°C).¹¹

1. *Bruker APEX2*, Bruker Analytical X-ray Instruments, Inc., Madison, Wisconsin, USA, 2005.
2. G. M. Sheldrick, in *Madison, WI*, Bruker Analytical X-ray Instruments, Inc., 2003.
3. A. L. Spek, *J. Appl. Crystallogr.*, 2003, **36**, 7-13.
4. G. H. Zhang, D. Xu, M. K. Lu, D. R. Yuan, X. Q. Wang, F. Q. Meng, S. Y. Guo, Q. Ren and M. H. Jiang, *Opt. Laser Technol.*, 2001, **33**, 121-124.
5. A. Bravais, *Etudes Crystallographiques*, Academie des Sciences, Paris, 1913.
6. J. D. H. Donnay and D. Harker, *Am. Mineral*, 1937, **22**, 446-467.
7. R. Taylor and C. F. Macrae, *Acta Crystallogr., Sect. B: Struct. Sci* 2001, **57**, 815-827.
8. I. J. Bruno, J. C. Cole, P. R. Edgington, M. Kessler, C. F. Macrae, P. McCabe, J. Pearson and R. Taylor, *Acta Crystallogr., Sect. B: Struct. Sci* 2002, **58**, 389-397.
9. D. R. Yuan, D. Xu, M. G. Liu, F. Qi, W. T. Yu, W. B. Hou, Y. H. Bing, S. Y. Sun and M. H. Jiang, *Appl. Phys. Lett.*, 1997, **70**, 544-546.
10. X. L. Duan, D. R. Yuan, X. Q. Wang, X. F. Cheng, Z. H. Yang, S. Y. Guo, H. Q. Sun, D. Xu and M. K. Lu, *Cryst. Res. Technol.*, 2002, **37**, 446-455.
11. D. R. Yuan, D. Xu, G. H. Zhang, M. G. Liu, S. Y. Guo, F. Q. Meng, M. K. Lv, Q. Fang and M. H. Jiang, *Chin. Phys. Lett.*, 2000, **17**, 669-671.